

Supporting information

Smart Mobile Pouch as a Biomechanical Energy Harvester towards Self-Powered Smart Wireless Power Transfer Applications

Arunkumar Chandrasekhar,^a Nagamalleswara Rao Alluri,^b M.S.P Sudhakaran,^c Young Sun Mok,^d Sang-Jae Kim^{ab*}

^a *Nanomaterials and System Lab, Department of Mechatronics Engineering,
Jeju National University, Jeju 690-756, Republic of Korea*

^b *Faculty of Applied Energy System, Department of Mechanical Engineering,
Jeju National University, Jeju 690-756, Republic of Korea*

^{c,d} *Department of Chemical and Biological Engineering Jeju National University,
Jeju 690-756, Republic of Korea*

^d *Department of Chemical Engineering, Pennsylvania State University, University Park, PA 16802-4400, U.S.A*

*Corresponding author: Tel: +82-64-754-3715; Fax: +82-64-756-3886

Email:kimsangj@jejunu.ac.kr;

Table of Contents

| | |
|------------------|---|
| Table S1 | Comparison of the proposed SMP-TENG with other reports |
| Figure S1 | Fabrication process of the SMP-TENG |
| Figure S2 | FE-SEM images of triboelectric active layer |
| Figure S3 | Triboelectric series of materials |
| Figure S4 | Typical electrical output performance of the plasma untreated SMP-TENG |
| Figure S5 | Stability test of SMP-TENG |
| Figure S6 | Real time energy harvesting and self-powered applications of SMP-TENG |
| Figure S7 | Photograph of wireless power transmission antenna |
| | (a) 30 turns antenna (b) 10 turns antenna |
| | (c) - (d) Voltage signal obtained during $T_x L_1 > R_x L_2$ and $T_x L_1 < R_x L_2$ |
| | at various transmission distance |
| | (e) Photograph of wireless power transmission and reception setup to charge a |
| | Li-ion battery |
| | (f) Wireless charging of Li-ion battery |

DBD plasma treatment (Dielectric Barrier Discharge): It is an electrical discharge between two electrodes separated by an insulating dielectric barrier. This process is named as silent (inaudible) discharge and also known as ozone production discharge.¹ The dielectric barrier discharge is created in the energetic plasma and reactive mono-atomic atmosphere, where a molecular diatomic charged particles, electrons and neutrals derived from the gases present. The plasma is also photon rich, with significant levels of ozone. The polymer surface during processing is exposed to a highly reactive regime. It has been shown that the reactive oxygen atoms produced by the dissociation of oxygen molecules in the discharge contribute mostly to the oxidative chemical effects during etching. At the same time, energetic plasma species cleave C-C and C-H bonds in the course of etching the upper surface layer of the polymer film undergoes the changes in the surface morphology.^{2,3}

In Figure S6 a (insets) the demonstration presents that the SMP-TENG is capable to harvest energy from low frequency human motion. The inset clearly presents the frequency of each human motion. Also from the above observations, SMP-TENG proves its reliability in bio mechanical energy harvesting. As the flash light in the mobile phone consumes more battery, while used as a torch light. Here we introduce a new self-powered application, which can be used in the emergency scenario. This self-powered emergency flash light was designed using SMP-TENG. A detailed circuit diagram is shown in figure S6 b, was constructed with a diode bridge rectifier (DF06G), capacitor ($C_1 = 20\text{nF}$), a press switch and a green LED array (50 LEDs). During the human motion an electrical signal is generated, this charge is stored in a capacitor (C_1). With respect to the human motion the charge stored in the capacitor and the time taken to charge varies, at once the switch is pressed the stored charge lit up the LED array which is connected to the circuit. Also with respect to the stored charge the intensity of the flash light varies. This integrated facility with the SMP-TENG will reduce the conception of mobile battery and extend the operation time of mobile phones.

Here, we propose an interesting application of SMP-TENG as a self-powered pedometer. It's an addition multi-feature of SMP-TENG, this demonstration shows the working of a self-powered pedometer to calculate the number of steps, speed of the motion and distance travelled. Figure S6 c presents the electrical signals obtained during walking motion, the cyclic peaks was acquired for each step of motion. Figure S6 d presents the voltage peaks for 131 steps obtained in 135 seconds. From the voltage signal we can calculate the distance travelled and speed of the motion using the following equation.

$$\text{Distance travelled} = \text{Walking steps} \times \text{Step length} \quad (1)$$

$$\text{Distance travelled} = 131 \times .52 \text{ m}$$

$$= 68.2 \text{ m}$$

$$\text{Speed of motion} = \frac{\text{Distance Covered}}{\text{Time taken}}$$

(2)

$$\text{Speed of motion} = \frac{68.2 \text{ m}}{135 \text{ sec}}$$

$$= .5 \text{ m/s}$$

Equation (1) denotes the distance travelled by the person and equation (2) denotes the speed of the motion. Apart, for a constant time period (10 s) we obtained various numbers of steps as presented in figure S6 e. Based on the equation (1) and (2) these data helps to find the distance travelled and speed of the motion for various numbers of steps at a constant time. The bar graph figure S6 f presents the

distance travelled and speed of the motion for 8, 12 and 16 steps. This demonstration clearly shows the potential of SMP-TENG as a self-powered pedometer.

Figure S7 a-b presents the digital photograph of wireless power transmission antennas with different number of turns 30 and 10 respectively. With respect to number of turns in antenna the voltage transmitted and received was varied. Figure S7 c-d presents the voltage obtained at the receiving antenna during $Tx L_1 > Rx L_2$ and $Tx L_1 < Rx L_2$ at various transmission distance between the transmitter and receiver antenna respectively. Inset shows the size difference of the transmitter and receiver antenna. Apart from this the distance between the $Tx L_1$ and $Rx L_2$ was varied approximately from 0 to 3 cm. Figure S7 e presents the photograph of wireless power transmission and reception setup to charge a Li-ion battery. Here, the distance between the TxL_1 and RxL_2 antenna were kept less than .25 cm to scavenge the maximum power transfer efficiency. The charged Li-ion battery lit up the LED connected to the circuit. Figure S7 f illustrates the charging curve of wirelessly charged Li-ion battery. The concept in this work launches a new approach in the field of commercializing the triboelectric nanogenerator as a consumer product.

| No | Device | Application | Mode of operation | Electrode material | Polymer material | Voltage | Current | Power | Power density | Ref |
|----|---------------------------------------|---|--------------------|--------------------|----------------------|--------------|------------------------------|-----------------|---|---------------------|
| 1 | Fully Packaged Blue Energy Harvester | Water wave energy harvester | Sliding | Al | PTFE | 120 V | 13.5 μ A | --- | 1.05 μ W/cm ³ (Only for TENG) | 4 |
| 2 | Single-Electrode-Based Rotating TENG | For Harvesting Energy from Tires | Sliding (rotating) | Al | PTFE | 55 V | --- | 30 μ W | --- | 5 |
| 3 | Highly reliable wind-rolling TENG | Operating in a wide wind speed range | Sliding (rotating) | Ag | Expanded Polystyrene | 11.8 V | 1.86 μ A | --- | --- | 6 |
| 4 | Self-cleaning hybrid energy harvester | Self-cleaning hybrid energy harvester | Sliding | ITO | PDMS | 7 V | 128 nA | 0.265 μ W | --- | 7 |
| 5 | SR-TENG | Self-powered contact area and eccentric angle sensors | Sliding (rotating) | Al | PTFE | 60 V | 20 μ A | 8.2 μ W | --- | 8 |
| 6 | A Ball-Bearing Structured-TENG | Nondestructive damage and rotating speed measurement | Sliding (rotating) | Cu | PTFE | 40 V | 1.2 μ A | 10.5 μ W | --- | 9 |
| 7 | SMP - TENG | Smart mobile pouch, Wireless power transfer | Sliding | Al | Kapton | 150 V | 305 μA | 0.021 mW | 0.13 mW/m² | Present work |

Table S1. Comparison of the proposed SMP-TENG with other reports

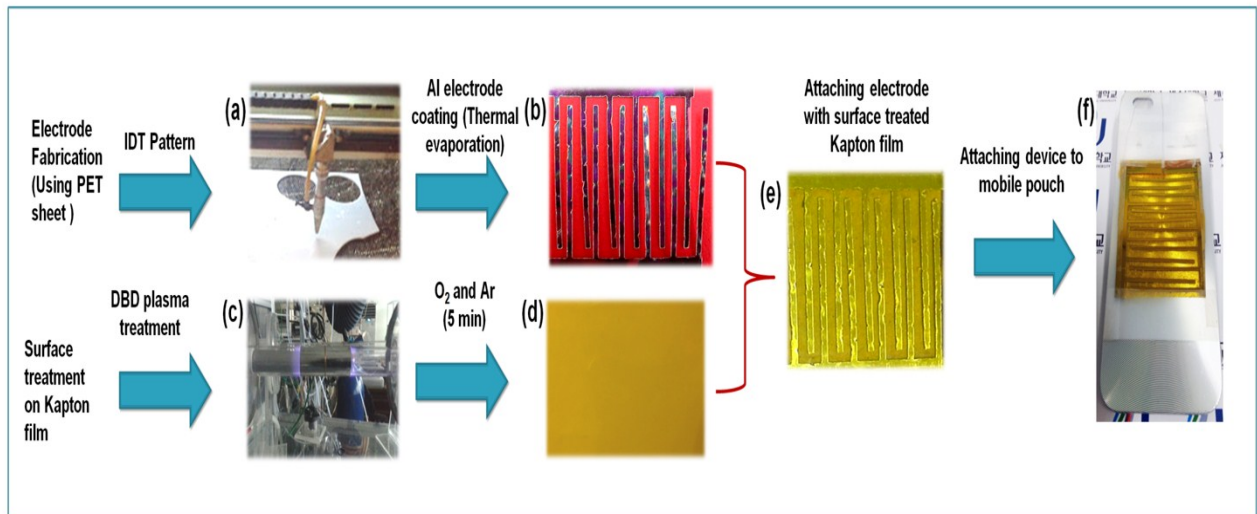


Figure S1. Fabrication process of the SMP-TENG. (a) Photograph of laser cutter, cutting IDT pattern on PET sheet. (b) Pre-patterned IDT structured PET sheet coated with Aluminum as electrode. (c) DBD plasma treatment for Kapton film. (d) Optical image of plasma treated Kapton film. (e) Surface treated Kapton film attached with the IDT electrode. (f) SMP-TENG attached to a mobile guard for physical support.

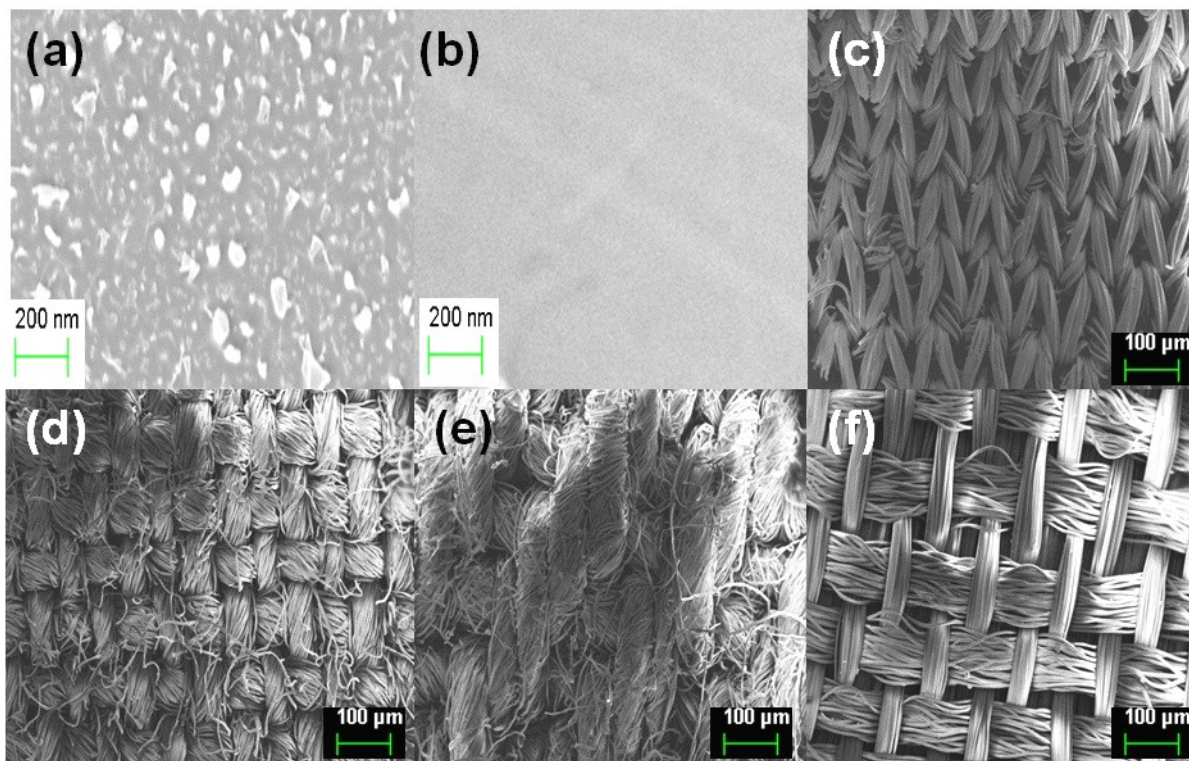


Figure S2. (a and b) FE-SEM images of triboelectric active layer: DBD plasma treated and untreated Kapton film. (c-f) Top view FE-SEM image of positively charged triboelectric contact materials: nylon, cotton, denim and polyester cloth.

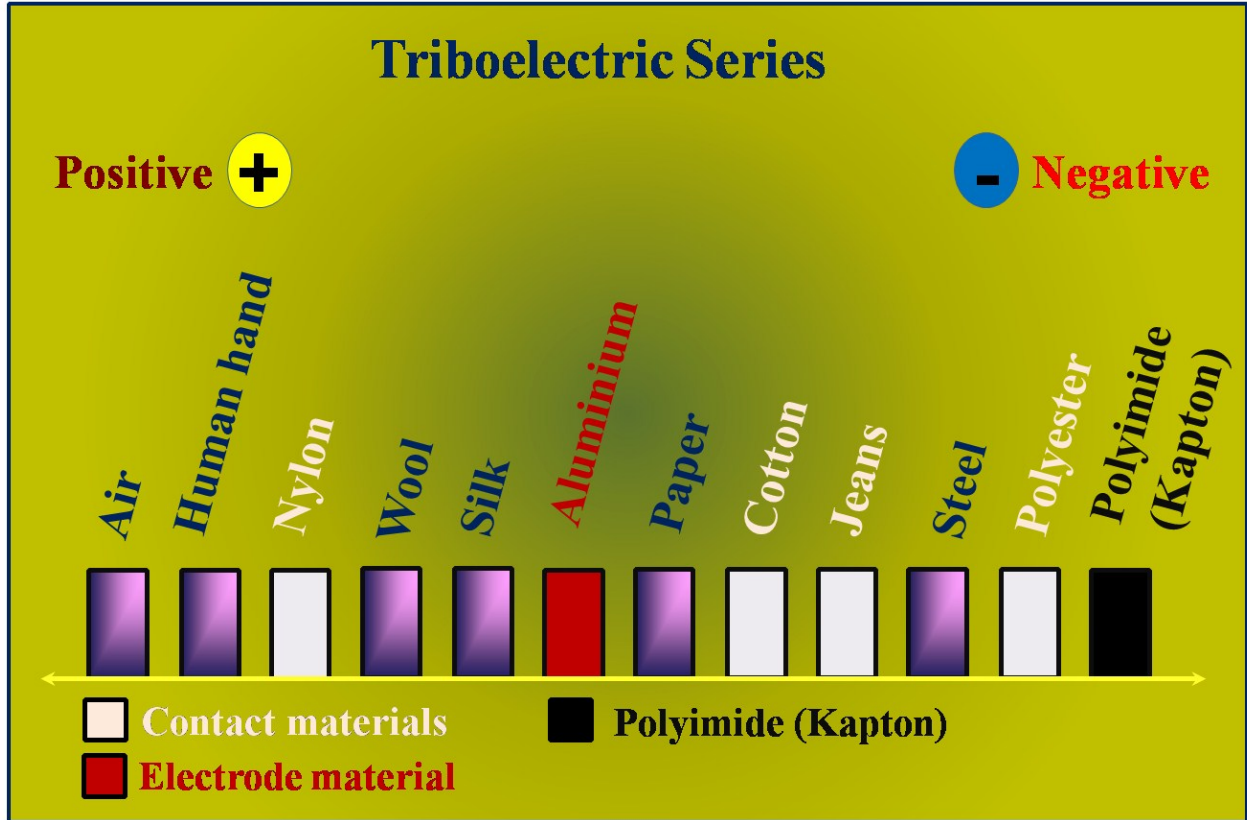


Figure S3. Triboelectric series: a list that rank various materials used for the SMP-TENG electrical studies, according to their tendency to lose electrons (positive) and gain (negative).

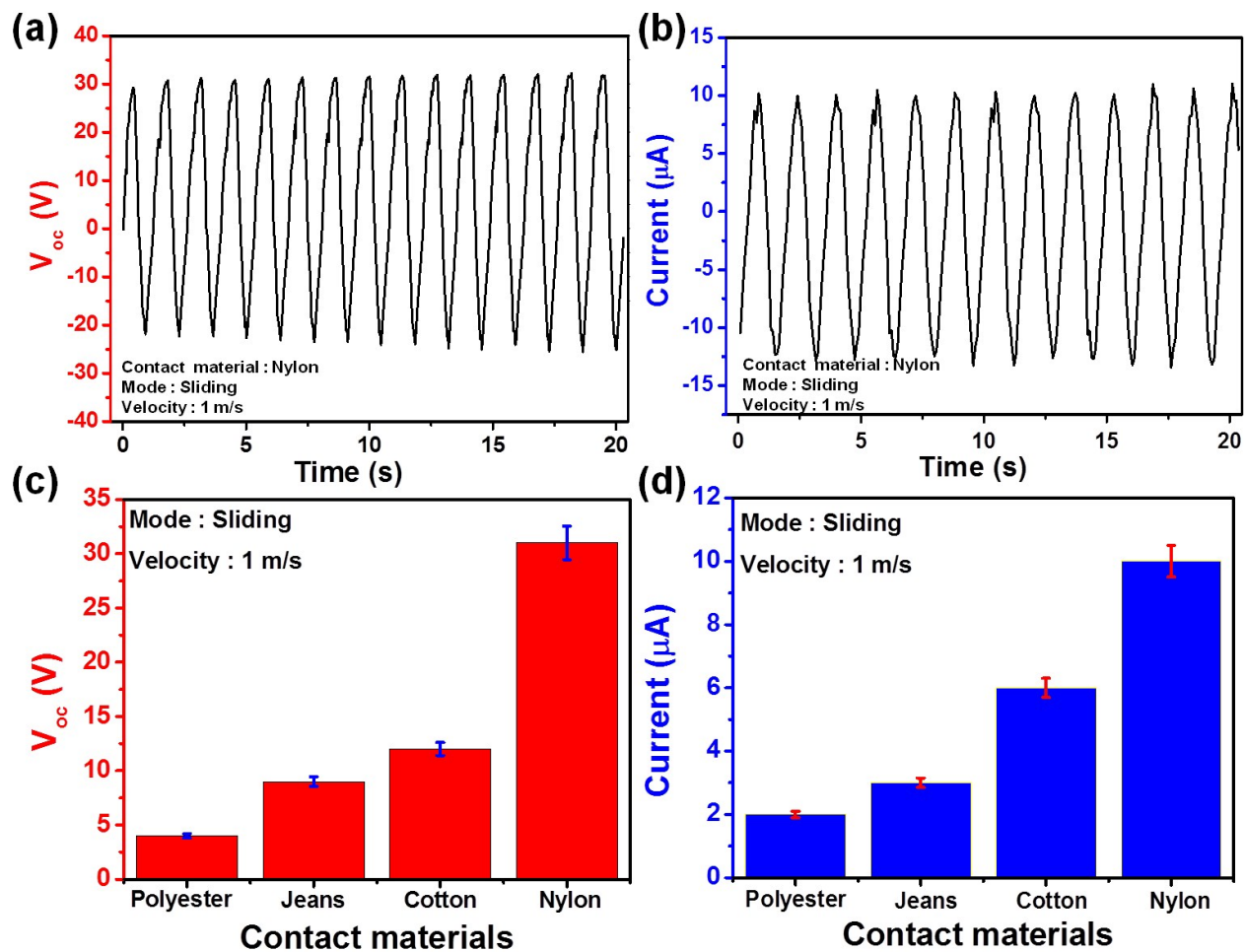


Figure S4. Typical electrical output performance of the plasma untreated SMP-TENG, sliding with different contact materials. (a) Open-circuit voltage and (b) short-circuit current of the plasma untreated SMP-TENG with nylon as a sliding material at a sliding velocity of 1 m/s. (c–d) Electrical response of the plasma untreated SMP-TENG with different freestanding fabrics (contact materials) at a sliding velocity of 1 m/s.

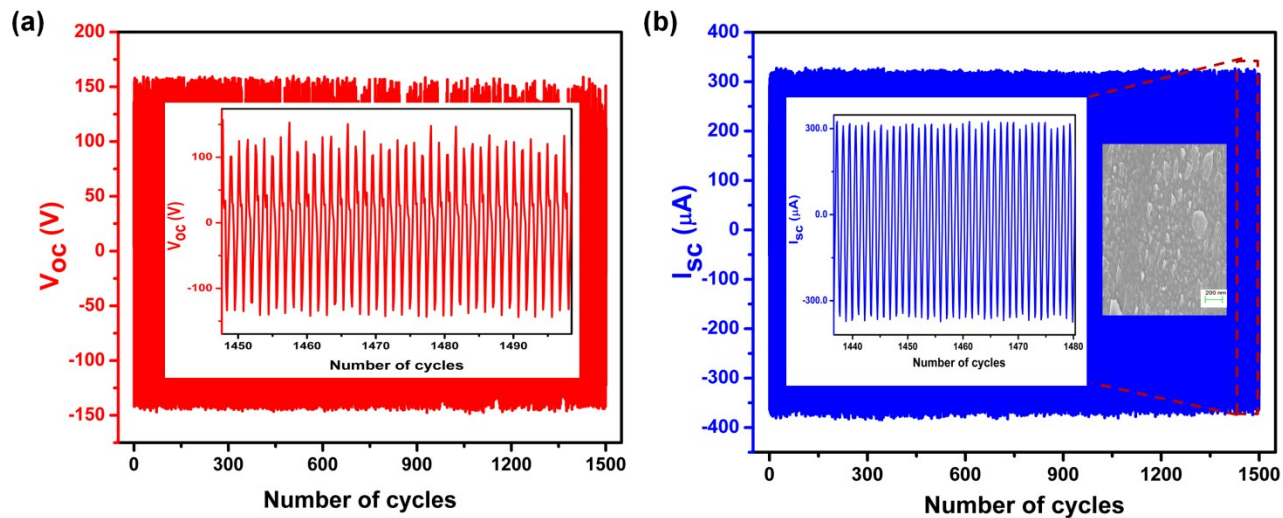


Figure S5. Stability test of SMP-TENG (a) Open circuit voltage and (b) Short circuit current. The inset shows an enlarged view of the electrical response at the end of the stability test and (inset) the FE-SEM image of the SMP-TENG after the stability test.

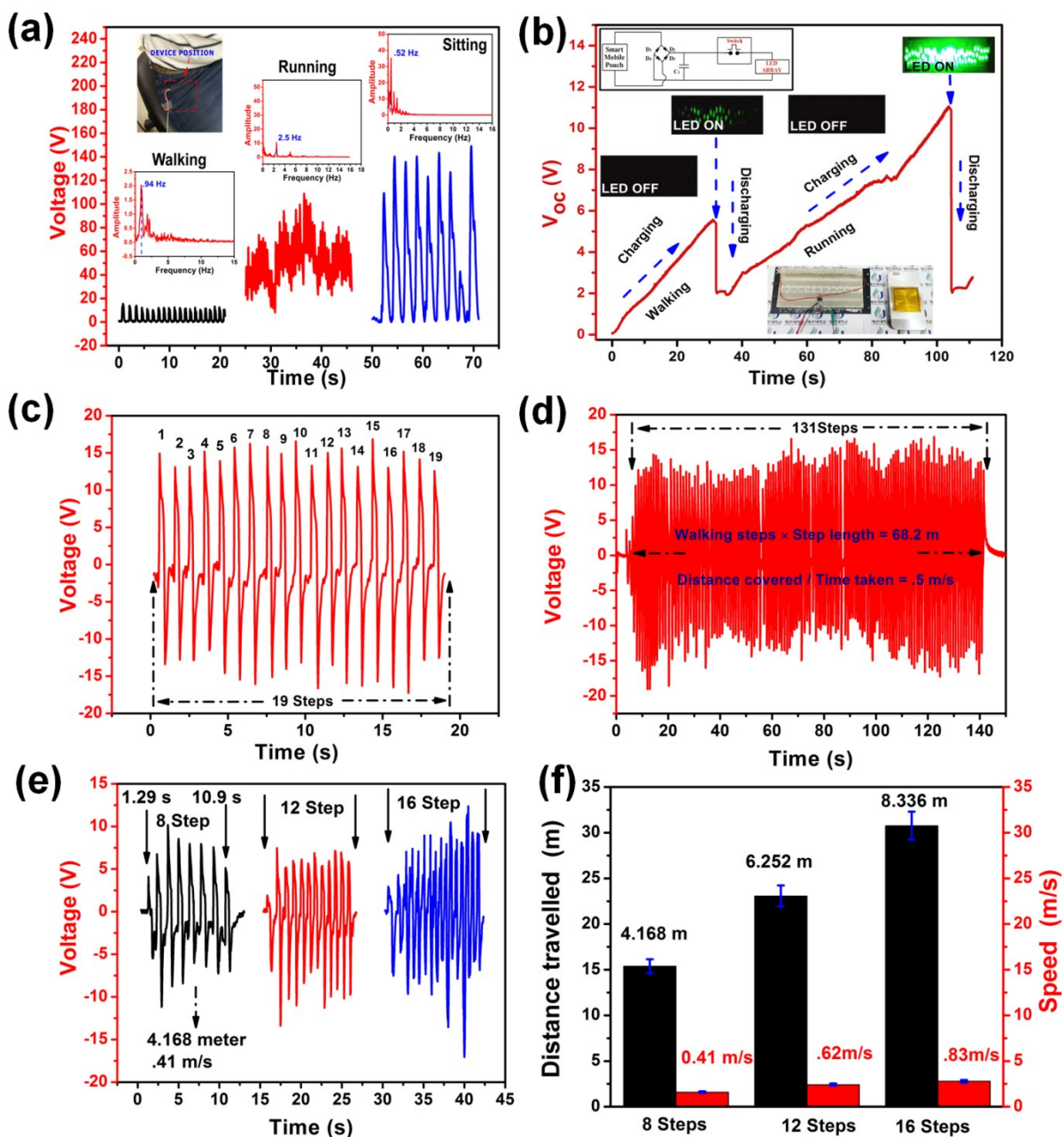


Figure S6. Real time energy harvesting and self-powered applications of SMP-TENG (a) Energy harvesting using SMP-TENG during a range of human motions. (Inset) The frequency domain after Fourier transformed of the harvested electrical signal during human motions. (b) Self-powered emergency flash light, powered during human motion. (Inset left) A circuit connection designed for self-powered emergency flash light and (inset right) photograph of SMP-TENG with self-powered

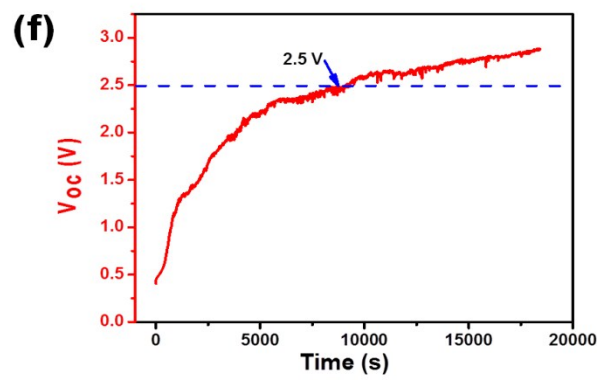
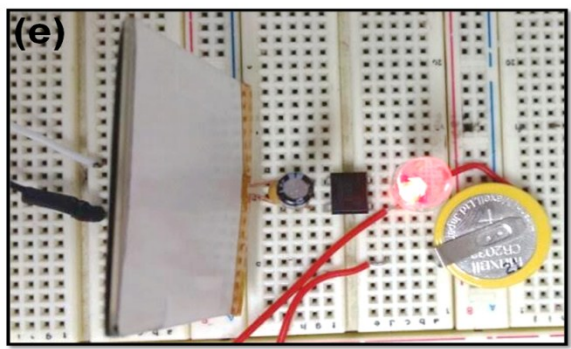
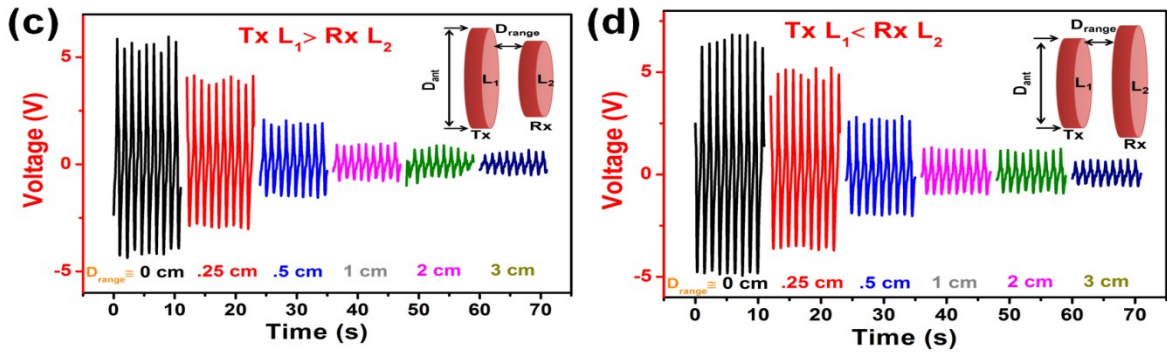
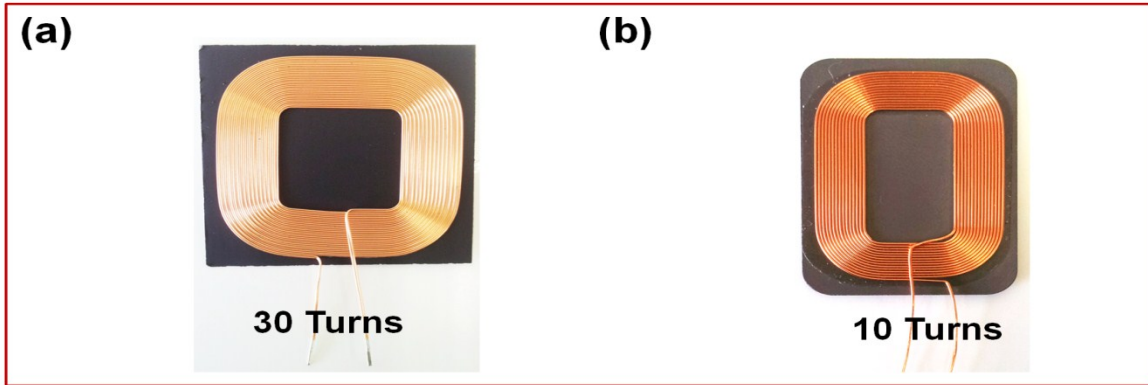


Figure S7. Photograph of wireless power transmission antenna. (a) 30 turns antenna (b) 10 turns antenna. (c)- (d) Voltage signal obtained at the receiving antenna during $Tx L_1 > Rx L_2$ and $Tx L_1 < Rx L_2$ at various transmission distance. (e) Photograph of wireless power transmission and reception setup to charge a Li-ion battery. (f) Wireless charging of Li-ion battery.

References

- 1 N.-Y. Cui and N. M. D. Brown, *Appl. Surf. Sci.*, 2002, **189**, 31–38.
- 2 H. C. Barshilia, A. Ananth, N. Gupta and C. Anandan, *Appl. Surf. Sci.*, 2013, **268**, 464–471.
- 3 F. Leroux, C. Campagne, A. Perwuelz and L. Gengembre, *J. Colloid Interface Sci.*, 2008, **328**, 412–420.
- 4 X. Wang, Z. Wen, H. Guo, C. Wu, X. He, L. Lin, X. Cao and Z. L. Wang, *ACS Nano*, 2016, **10**, 11369–11376.
- 5 H. Zhang, Y. Yang, X. Zhong, Y. Su, Y. Zhou, C. Hu and Z. L. Wang, *ACS Nano*, 2014, **8**, 680–689.
- 6 H. Yong, J. Chung, D. Choi, D. Jung, M. Cho and S. Lee, *Sci. Rep.*, 2016, **6**, 33977.
- 7 S.-B. Jeon, D. Kim, G.-W. Yoon, J.-B. Yoon and Y.-K. Choi, *Nano Energy*, 2015, **12**, 636–645.
- 8 Y. Li, G. Cheng, Z.-H. Lin, J. Yang, L. Lin and Z. L. Wang, *Nano Energy*, 2015, **11**, 323–332.
- 9 X. H. Li, C. B. Han, T. Jiang, C. Zhang and Z. L. Wang, *Nanotechnology*, 2016, **27**, 85401.